

V. V. Sobolev¹,
orcid.org/0000-0003-1351-6674,
S. M. Hapiev¹,
orcid.org/0000-0003-0203-7424,
O. V. Skobenko¹,
orcid.org/0000-0003-4606-4889,
V. V. Kulivar¹,
orcid.org/0000-0002-7817-9878,
A. V. Kurliak²,
orcid.org/0000-0002-9928-0406

1 – Dnipro University of Technology, Dnipro, Ukraine,
e-mail: velo1947@ukr.net
2 – Enterprise “Research-Industrial Complex “Pavlohrad
Chemical Plant”, Pavlohrad, Dnipropetrovsk Region, Ukraine

ON THE MECHANISM OF IONIZATION OF ATOMS AT COMPRESSION OF A SUBSTANCE BY FRONT OF THE CONVERGING SHOCK WAVE

Purpose. To study changes in the microstructure of metals after exposure to high-energy plasma jets formed by the cumulation of gas-dynamic flows in a conical target. To estimate the expected state of matter in a strong shock wave compression, taking into account the change in volumetric energy density at the moment of transformation of a solid body plasma into nuclear matter.

Methodology. The technique of laser initiation of a profiled front of detonation waves in explosive charges and the corresponding profile of shock waves in materials, methods and techniques for measuring the dynamic parameters of shock-compressed substances are used.

Findings. An experimental study on the physicochemical state of a substance that has been processed with extremely high pressures and temperatures during compression by converging shock waves in conical targets has been carried out. Scientific results of physical and mathematical modelling of converging shock waves are analysed.

Originality. For the first time, the formation of symmetric plasma jets during gas compression in conical targets has been experimentally observed. For the first time, metallo-physical studies on the microstructure of cast iron and steel have been carried out. These studies were made after the action of high-energy dense plasma jets with a temperature of $(2.5-2.8) \cdot 10^6$ K and a pressure $1.12 \cdot 10^{12}$ arising from the collision of the jet with a barrier. Iron-55 and copper-64 isotopes were found in the cast iron microstructure near the surface formed by the action of the plasma jet. The main components of the plasma jet were gaseous oxygen, nitrogen, argon, and atomic iron, copper and gold. The fact of formation of isotopes is the result of nuclear reactions. One of the main conditions for the implementation of such reactions is a dense high-temperature plasma. It is assumed that under the action of a strong shock wave in a conical target, in addition to the synthesis reaction, other nuclear reactions with heavy elements can be realized. The ideas about the expected state of matter in a compression shock wave are presented, taking into account the change in the volumetric energy density at the moment of transformation of a solid body plasma into nuclear matter.

Practical value. The proposed technique for conducting experimental studies on a shock-compressed substance under the action of extreme temperatures and pressures in conical targets using laser initiation of chemical explosives is of practical importance. The idea of the expected state of matter in the shock wave is also important.

Keywords: *explosion, shock wave, conical target, thermonuclear temperature, plasma, isotopes, nuclear reactions*

Introduction. The propagation of shock waves in a solid body is accompanied by physical and chemical changes in the substance at the microstructural, atomic and electronic levels. The electrical, magnetic and optical properties of solids change, phase and polymorphic transitions, the polymerization of matter occur. Depending on the intensity of shock waves and the properties of the initial substance, the structure and properties of the internal interfaces change, the crystal grains are fragmented, the valence changes, new phases are formed, and the density of defects in the crystal structure increases, the internal energy of the crystal and other physicochemical properties is growing. One of the main reasons causing various physicochemical transformations in condensed media is, in particular, the peculiarity of shock-wave processes, which consists in an abrupt increase in pressure in the shock wave front over times of $10^{-11}-10^{-12}$ s. The physical and chemical features of the transformations in each of the substances manifest themselves depending on the magnitude of the acting shock pressure, which, according to the type of transformations and the final state of the substance, can be classified as low, medium, high, and ultrahigh.

Literature review and unsolved aspects of the problem. Of the greatest scientific interest is the action of ultrahigh concentrations of energy (thermal, mechanical, electromagnetic, etc.) on matter as a factor capable of initiating the complete

destruction of electron shells [1], the decay of properties of the substance [2], the formation of dense plasma [3, 4], isotopes and new chemical elements [5–7] that are absent in the original substance.

From the point of view of practical use associated with the search for new sources of energy, the greatest attention is paid to the physical processes of the formation of new chemical elements. For the first time, these effects manifested themselves in metals as a result of the penetration of microparticles to great depths [8, 9], superstrong compression of matter by converging cylindrical [10] or spherical shock waves [11, 12], in studies on the shock-wave initiation of the D-D reaction and the yield of neutrons in conical targets [4, 13], in experiments on gas compression in conical cavities [14], and study on the effect of plasma jets on the metal structure [15].

Achieving high and extreme values of various physical parameters, obtaining them by simpler methods, in various combinations, largely determines the development of many important areas of science and technology, especially in the field of energy and materials science.

At the beginning of this century, articles about the results of research by the “Proton-21” laboratory of the Institute for Nuclear Research of the National Academy of Sciences of Ukraine periodically appeared in the media. Converging shock waves were obtained in metals when studying an electric vacuum discharge in a pulsed mode with a duration of the order of several nanoseconds in an anode in the form of a ball or a cylindrical shape [10–12]. Near the centre or axis, a plasma

was obtained with a concentration of atomic nuclei exceeding $n > 10^{33} \text{ m}^{-3}$. At the same time, the upper estimates of the concentrations of nuclei reached values $n \sim 10^{36} - 10^{39} \text{ m}^{-3}$, which are relatively close to the density of nuclear matter, $n_n \sim 10^{44} \text{ m}^{-3}$. Electron bombardment of a copper anode near the centre of a converging shock wave results in the synthesis of nuclei of many isotopes of known chemical elements, including unknown superheavy elements. The ratio of the energies released to and put in the pulse reaches 5–7 orders of magnitude, which coincides with similar estimates given in [5, 7]. It is likely that a medium consisting of a dense plasma is necessary for the implementation of such reactions. Despite the long-term efforts of experimental studies using particle accelerators (without the participation of electrons in reactions), such processes have not been implemented yet.

The fundamental possibility of nuclear transformations at the point of converging high-energy flows of multiply charged ions (at the plasma focus) was also pointed out earlier [4, 16, 17]. The short-term and extremely powerful X-ray, light and gamma radiation observed in [18, 19] were also recorded in studies on the stability of the microstructure of metal barriers under the impact of a high-speed flow of microparticles [20]. In [21], the authors found the formation of chemical elements in the microstructure of a massive iron barrier as a result of the penetration of metal microparticles into it to depths from several tens to two hundred millimetres.

The analysis of research results of the mechanism of ultra-deep penetration of microparticles into metals and electromagnetic effects accompanying microparticles penetrating into metal targets to ultra-great depths [8, 21], the parameters of plasma jets in closed conical cavities [4, 13], the fundamental possibility of recycling radioactive materials [22] and low-energy nuclear transformations [23] makes it necessary to resolve a physical contradiction. The main contradiction is that the energy expended is $10^5 - 10^7$ times less than that required for the formation of new isotopes. Various scenarios of supposed low-energy nuclear transformations are characterized by such physical conditions and factors as electron in initiation of nuclear reactions [24, 25], nuclear fusion [26, 27], electron catalysis (in chemical reactions) [28], and others discussed in [27, 29].

The effect of gas-plasma jets formed in closed conical cavities on the microstructure of metals was reported in [30], but the information was inadequate from the point of modern ideas about nuclear, physical and chemical processes. According to estimates [26], the temperature of the plasma jet is in the range from $3.4 \cdot 10^5$ [15] to $1.7 \cdot 10^6$ K [31]. In conical cavities (conical targets), the authors of [4, 12, 13] report a neutron yield at a level of $10^4 - 10^9 \text{ pulse}^{-1}$. The formation of isotopes in the microstructure of metal elements of conical plasma generators and the possible mechanism of isotope formation have not been studied.

Thus, the **purpose** is to study the change in the microstructure of metals after exposure to high-energy plasma jets formed by the cumulation of gas-dynamic flows in a conical target and to estimate the expected state of matter in a strong compression shock wave, taking into account the change in volumetric energy density at the moment of transformation of solid-state plasma into nuclear matter.

Materials and methods. Experimental studies were carried out at the test site of the State Enterprise Research-Industrial Complex "Pavlohrad Chemical Plant". In the experiments, we use a device that creates high pressure in the material under study by hitting a metal plate accelerated by the detonation products of an explosive. In the device, Fig. 1, an HMX charge with a detonation velocity of 8,590 m/s was used. Adjacent to the open base of the explosive charge is an initiating layer made of a photosensitive explosive composite (PEC), the characteristics of which are studied in [32], as well as experimental PEC samples synthesized on the basis of lead azide. PECs were used to form a flat profile of the detonation wave in the explosive charge.

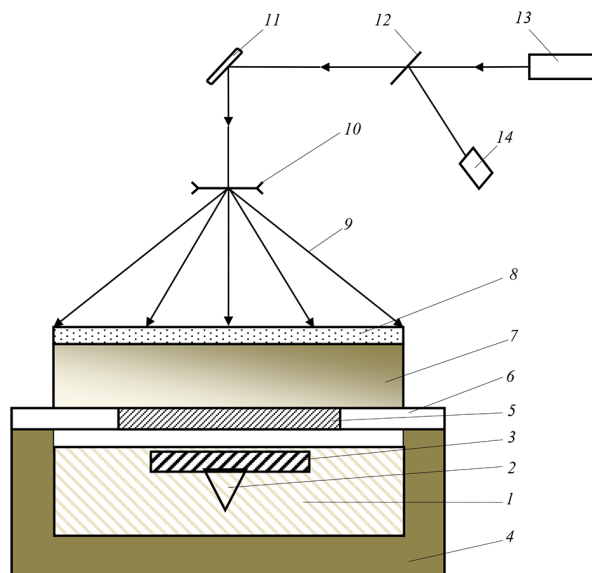


Fig. 1. Diagram of an explosive generator that forms a flat front of a detonation wave in an explosive charge:

1 – steel matrix; 2 – conical target; 3 – cast iron plug; 4 – lead matrix; 5 – steel plate-striker; 6 – ring; 7 – explosive charge; 8 – photosensitive explosive composite; 9 – extended laser beam; 10 – divergent lens; 11 – prism; 12 – mirror; 13 – optical quantum generator; 14 – laser diode for laser beam alignment

The detonation of the initiating layer of the PEC was carried out by the action of pulsed radiation from a neodymium glass laser (laser energy 0.17 J , radiation time $11 \cdot 10^{-9} \text{ s}$ at half-height of the laser pulse maximum; wavelength $1.06 \cdot 10^{-6} \text{ m}$). To initiate simultaneously the entire surface of the open base of the PEC, the laser beam was expanded using a lens [33] to the layer diameter. The method for forming a plane detonation wave is reliable. Evidence is a number of positive experimental results obtained during the formation of plane shock waves in the material under study directly by a plane detonation wave front at an angle of 0° relative to the surface of the material facing the striker [33, 34], or by a detonation wave front sliding at an angle of 90° to the generatrix of the cylinder surface [35], or by the impact of a flat plate accelerated by the products of the PEC explosion [36], including in problems of studying the nature of the flow of matter behind the front of the bow shock [37].

Devices and methods for accelerating flat strikers by explosion products, methods for measuring the dynamic compressibility of materials [13] were used in the work. Methods are based on determining the velocity of propagation of shock waves (D) and the mass velocity of particles behind the wave front (u) [38]. Methods for increasing the acceleration rate and registration of flat metal striker plates [39], which create pressures of the order of 1011–1013 Pa and higher during compression of the substance under study were used as well [40, 41].

The steel matrix with a conical target (as well as the striker plate) is made of low-carbon steel in the form of a disc 40 mm thick, 80 mm in diameter. In the disk, on the side of the base facing the striker plate, a cylindrical cavern is made (15 mm deep, 30 mm in diameter), having a conical depression at the base (cone height 3.0 mm, diameter 6 mm, cone opening angle $\sim 90^\circ$; apex cone coincides with the axis of the steel sample); the volume of the cone is $42 \cdot 10^{-9} \text{ m}^3$. The angle between the plane shock wave front entering the cone and the generatrix of the cone, 45° , was within the range of angles $39 - 55^\circ$, corresponding to the angles of irregular reflection of shock waves in air [42]. The physical features of shock wave flows in a cone illustrate convincingly the results of physical and mathematical modelling [43], from which one can see the scenario of the formation of primary and secondary Mach waves as one of the most significant parameters of increasing pressure on substances [44].

To quantify the metal mass in the resulting plasma jet and estimate the jet density, gold and copper coatings were deposited consecutively on the inner surface of the conical target, each layer up to 3 μm thick. For this purpose, a WUP-4 vacuum post was used. The cylindrical cavern in the sample was closed with a stopper (thickness 15 mm, diameter 30 mm) made of ferritic cast iron (iron – 92.261, carbon – 3.06, nickel – 4.32, sulphur, manganese, silicon and other elements – 0.359 %) with plate-like graphite inclusions. The isotopic and chemical composition of the elements was determined using a MI-1201AT-01 mass spectrometer.

One way to increase the gas temperature behind the shock wave front is to add argon to the gas filling the conical target (the process was modelled by K. Yakh, 1977). This work uses not only the idea, but also the methodology for conducting experiments (Gao K., Jach K. & Kaliski S., 1978). The addition of argon increases the temperature of the deuterium plasma and the neutron yield by more than 30 times. From the dependences “gas temperature – shock wave velocity” given in [45], it follows that with a decrease in the energy of the first ionization of atoms of inert gases, their temperature increases during shock compression, Fig. 2. The equations of state for argon and air are taken from [46, 47]. Data for argon given by V. E. Fortov, A. A. Leontiev, A. N. Dryomin, V. K. Gryaznov (1976) and in [48–50] are valid in the pressure range from 1.0 to $4 \cdot 10^{10}$ Pa, temperatures up to 10^5 K, and $n_e \sim 10^{14} - 3 \cdot 10^{21}$ cm^{-3} . With these parameters, developed ionization ($\alpha \sim 3$) and strong Coulomb interaction ($\Gamma \sim 10^{-2} - 5.2$) are realized. For argon gas, the speed of sound is $c_0 = 308$ m/s, the initial density is $\rho_0 = 1.78$ kg/m^3 . The numerical values of the coefficients of the shock adiabat written in the form $D = A + Bu$ for air (speed of sound $c_0 = 308$ m/s, initial density $\rho_0 = 1.29$ kg/m^3) are as follows: $A = 269$ m/s, $B = 1.046$ [13].

When creating the dynamic compressibility and equations of state of substances, well-known methods are used, given in the first publications of V. G. Walsh (1955), D. Bankroft (1955), W. Goranson (1955), L. Altshuler (1958–1962). For the experimental determination of the dynamic parameters, the “braking” method described in [51] was used.

An increase in the temperature of the gas filling the cavity increases the probability of metal ablation from the surface of the conical target, increasing the density of the jet (A. Ye. Voytenko, 1964, 1966). In addition, when a shock wave reaches the free surface of a cast-iron plug adjacent to the base of the conical cavern, a finely dispersed fraction of particles is ejected from the surface of the plug into the conical cavern [52]. Although this effect (except for the studied particles with a size of 1 μm or more) does not yet have data on the magnitude of the flow mass as a whole, the contribution to the increase in the jet density can be noticeable.

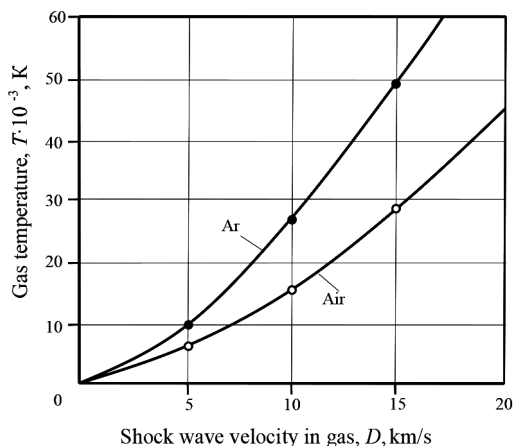


Fig. 2. Dependence of gas temperature change on the velocity of the shock wave front

Research results. The change in the state of matter after shock compression is described using the laws of conservation of mass, momentum, and energy [51]. Applying these laws, the thermodynamic properties of a substance are expressed, in particular, in the form of a one-parameter kinematic dependence $D_{sw} = f(u)$, where D_{sw} is the shock wave front velocity, u is the mass velocity of matter particles behind the shock wave front. The values of the coefficients A and B are found in the equation $D_{sw} = A + Bu$, which relates the velocity of propagation of the shock wave and the mass velocity of particles behind the wave front. For cast iron, having a density $\rho_0 = 7,683$ kg/m^3 , $A = 3,859$; $B = 1.566$; for steel (density $\rho_0 = 7,850$ kg/m^3) $A = 3,816$; $B = 1.578$.

The speed of the steel plate at the moment of impact on the cast-iron plug was 10,450 m/s. Insignificant differences between the coefficients A , B for cast iron and steel can be neglected when estimating the pressure at the collision boundary (plate – plug) and the mass velocity of particles behind the shock wave front. In this case, when an incoming steel plate strikes cast iron, the mass velocity of particles behind the shock wave front will be equal to half the velocity of the plate, i. e., 5,225 m/s. The speed of the shock wave front in a cast-iron plug is $D_{sw} = 3,859 + 1.566 \cdot 5,225 = 12,041$ m/s. The calculated pressure in the plate will be $4.94 \cdot 10^{11}$ Pa, in the plug – $4.83 \cdot 10^{11}$ Pa, i. e. the indicated values differ by 2.3 %.

Estimation of the temperature during gas compression by a metal piston entering a conical cavity was carried out using the methods proposed in [6, 26, 31]. The estimates of the temperature of the compressed gas, the plasma jet, and the pressure of the jet on a metal barrier did not take into account a number of effects, such as the contribution of equilibrium radiation to the total thermodynamics of matter at the temperature $T = 10^7$ K, relativistic effects, which become important at a temperature of the order of 100 keV. When a flat front of an incoming shock wave propagates with a velocity of $D_{sw} \sim 13$ km/s, the temperature of argon behind the front increases to 3,700 K, and of air, to 16,000 K, Fig. 2. We will call such a rise in temperature the first shock wave and an increase in the temperature of the medium.

The second temperature jump behind the front of the primary Mach wave, the formation of which is typical for devices with cylindrical symmetry [53], has physical features. In devices that are conical targets [13, 14], wedge-shaped cavities [4, 54], or known designs of Voytenko generators [15, 45], irregular reflections of shock waves occur with the formation of a three-wave shock configuration in devices with cylindrical symmetry of elements (G. A. Adadurov, S. S. Batsanov, O. N. Breusov, A. A. Deribas, A. N. Dryomin, S. V. Pershin, A. M. Staver (1965–1979).

A rough estimate of the pressure of the plasma jet on the steel barrier will be obtained using the expression given in [42]

$$P = 4/3(\rho u^2),$$

where $\rho = 15,300$ kg/m^3 is plasma jet density; $u = 23,400$ m/s is jet speed.

The jet pressure on the barrier is $P = 1.12 \cdot 10^{12}$ Pa. The order of magnitude of the pressure that occurs when the jet hits the barrier gives reason to assume that the media in the impact zone were in the state of a degenerate gas [42]. The well-known heat capacity formula for a degenerate electron gas is used to estimate the temperature. Due to the fact that the density and atomic weight of the jet had estimated values, then, accordingly, the temperature values will be in a certain range of values $(2.5 - 2.8) \cdot 10^6$ K.

Studies on shock-compressed metals were carried out two hours after the explosive impact. A steel target with a cast-iron plug was cut along the axis. Cavities formed in the plug and target, which, relative to the top of the conical depression, coincided with the axis of the depression, but were oppositely directed, Fig. 3, a. The only reason for the formation of symmetrical cavities is the action of high-temperature plasma jets.

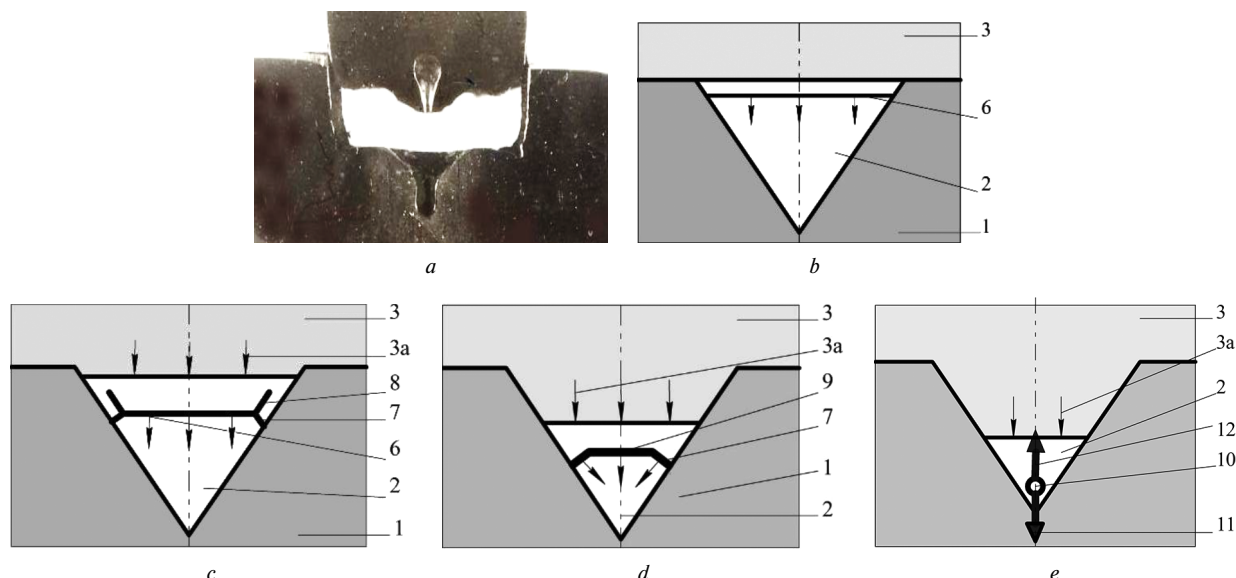


Fig. 3. Diagram of the proposed shock-wave flow in a conical target:

1 – steel sample with a conical target (2); 3 – cast iron plug; 3a – direction of motion of the plug surface; 4 – cavity (crater) in a steel sample; 5 – cavity (crater) in a cast-iron plug; 6 – incoming wave front (IS); 7 – primary Mach wave (MS1); 8 – reflected wave (RS); 9 – secondary Mach wave (NS2); 10 – plasma focus (PF); 11, 12 – symmetrical plasma jets

The diameter of the cavity formed by the action of the jet in the cast-iron plug noticeably decreases towards the lower base. This is owing to the fact that after the completion of the jet action, the filling of the conical target with the plug material continued for some more time.

Taking into account the results of similar studies and numerical modelling of converging shock waves presented in the works by A. Voytenko, V. Belokon, S. Anisimov, G. Romanov, E. Popov, I. Lomonosov, I. Sokolov, V. Fortov, A. Charakhchyan, S. Kaliski, K. Yakh, H. Derentovich and many other specialists, a simplified diagram of the expected way of the interaction of shock waves in a conical target is shown in Figs. 3, b, c, d, e.

Fig. 3, b shows the start of shock wave propagation from the iron-gas interface and the direction of movement of its front in the gas. Behind the wave front, the density, pressure, and temperature of the gas increase abruptly. The conical target in this case can be represented as a part of the ball bounded by the surface of the cone. The base is the base of the segment, and the top is the centre of the ball. After the wave front is reflected from the iron-gas interface, a dilution wave propagates in the plug, and at this moment the plug material begins to move, flowing into the conical cavity.

Configuration as a result of irregular reflection of the front of the incoming shock wave from the side surface of the conical target. As a result of this interaction, a configuration is formed consisting of an incoming wave (IS), a reflected wave (RS), and a primary Mach wave (MS1). The pressure in the Mach wave front is several times higher than the pressure in the wave front entering the cone cavity (Glass I., 1974) [55]. The problem of cumulation of shock-wave flows during compression of a spherical (or conical as a special case) front of a detonation wave was first considered by Ya.B. Zeldovich (1959), who showed the effect of cumulation of converging waves, resulting in an increase in the mass velocity of particles behind the wave front, the density and temperature of the substance.

Fig. 3, c shows the formation of a three-wave shock Fig. 3, d shows the moment of disappearance of the plane front of the incoming wave and the reflection of the primary Mach wave from the axis of symmetry. Reflection gives rise to a secondary Mach shock wave. Thus, the movement of the primary and secondary Mach waves is directed towards the top of the cone. A metal piston, flowing into the cone of the cork material, car-

ries out additional compression of the substance filling the target. As plasma flows approach the top of the cone, the degree of amplification of the shock-wave parameters of the medium increases.

A feature of the final stage of the process of compression of matter at the top of the cone, Fig. 3, e, is the collision of plasma flows converging to the top of the cone, formed behind the Mach waves. In the plane, the shock-wave flow is two plasma flows colliding at an angle, as a result of which two symmetrical plasma jets are formed, oppositely directed and coinciding with the axis of symmetry. According to A. Voytenko, the plasma density is $15,300 \text{ kg/m}^3$. The velocity of the jet exceeds the collision speed of the Mach waves and the plasma flows following them. In this case, the increase in the energy density of plasma jets is due to the redistribution of the energy of the medium during its motion [4]. In the collision area of plasma flows, a so-called plasma focus is formed, in which the maximum degree of cumulation of the energy of the medium is realized and there is a jump increase in temperature and ion concentration.

The study on structural transformations was carried out in the microstructure of a cast-iron plug and a metal target adjacent to the corresponding cavities. A cavity formed on the side of the lower base of the plug, Fig. 4, a. As a result of the action of high temperatures and pressures, an area of structural changes is located around the surface of the cavity, which differs from the initial microstructure of grey ferritic cast iron, Fig. 4, b, and consists of two zones. The first zone is adjacent directly to the cavity and consists of melted material. There was a crushing of coarse graphite inclusions to fine particles less than $2 \mu\text{m}$ in size and their redistribution in the molten layer in its microstructure. Development of vortex flows is observed, Figs. 4, b, c. Numerous disturbances of the continuous micron-scale structure are observed, which indicates a high cooling rate (of the order of 108 K/s). In general, the maximum width of this zone is in the range of $300\text{--}420 \mu\text{m}$, Fig. 4, d, and decreases to a minimum of $50 \mu\text{m}$, Fig. 4, e. Mass spectroscopic analysis revealed iron-55 and copper-64 isotopes in this zone.

The original structure was preserved in the second zone of structural changes in cast iron, but plastic flow of the metal occurred. Slide lines are visible in the cast iron matrix, especially strongly developed at the base of the cavity, Fig. 4, d. The slide lines are strongly curved due to turbulent flows in the

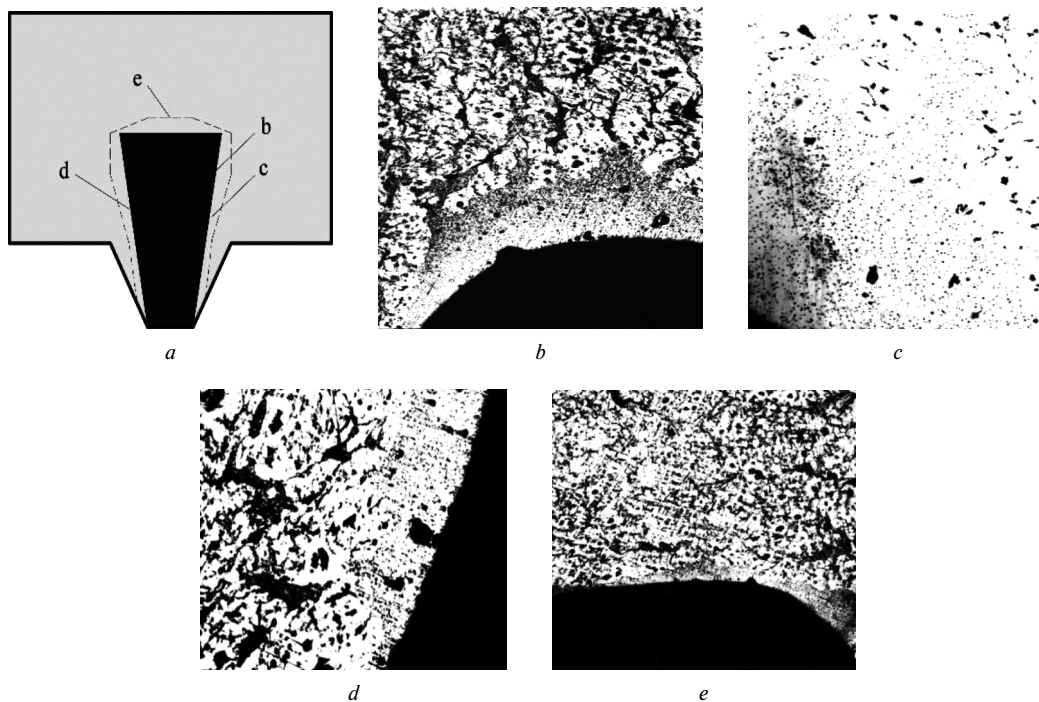


Fig. 4. Cast iron microstructure near a cavity formed by high-energy gas-plasma jets:
b, d, e – ×50; c – ×100

cast iron matrix, which led to the development of rotational deformation. It is associated with a change in the spatial orientation of local regions of crystals because of the movement of dislocations. Thus, the strain-hardening zone is characterized by the development of shear and rotational deformation components. Vortex flows in the cast iron matrix structure led to distortion and redistribution of graphite inclusions. Near the upper edge of the cavity, the graphite inclusions reoriented almost in the horizontal direction (Fig. 4, *e*), which, in our opinion, is associated with a decrease in the kinetic energy of the jet, which, spreading to the sides, washed out the metal in

the cast iron matrix. Isotopes of iron-55 and copper-64 were found in the zone shown in Figs. 4, *d, e*.

In the first zone (melting zone), the microhardness of the metal exceeds the microhardness of the original cast iron by 2.53 times. In the zone of strain hardening, the microhardness of cast iron after explosive action increased by 1.4 times.

The collision of plasma flows in the region of the top of the conical target resulted in the formation of a dense plasma. The jet penetrated to a depth of 9 mm, resulting in a cavity close to the shape of a cylinder. In the steel sample, a white layer 10 to 110 μm thick adjoins the base of the cylindrical cavity (Figs. 5, *e, c*). The

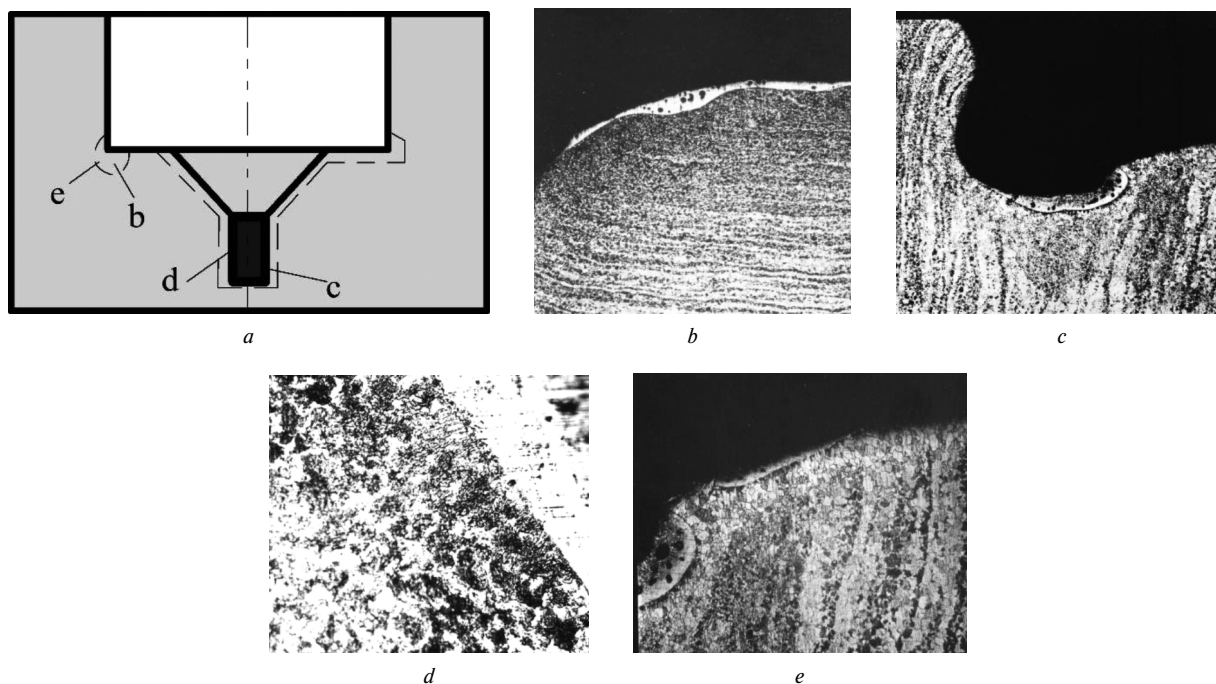


Fig. 5. The microstructure of steel in the zone of interaction with the plasma jet:
b, c – ×500; d – ×400; e – ×100

microstructure of the white layer is gardenite, which is characterized by ultrafine granularity and significant distortions of the crystal lattice. The appearance of the white layer is associated with the release of significant energy during the transition of the shock wave at the boundary between the iron plug and the steel sample, which caused the melting of the steel sample layer. The many gas bubbles in the layer, in particular, evidence this. Microcracks of thermal origin appeared near non-metallic inclusions in the microstructure, Fig. 5, *d*. The isotopes ^{55}Fe and ^{64}Cu were found in the zone, the possible mechanism of their formation will be discussed below.

A heat-affected zone was revealed in the steel microstructure. As a result of heating to the temperature of austenite formation and subsequent cooling in this region adjacent to the white layer, the streaky nature of the structure disappeared, and the steel became decarburized, Fig. 5, *e*. The width of the decarburization zone ranges from 50–60 μm . During the impact, the carbon content decreased from 0.4 % to a value that ensured the formation of a purely ferritic structure. The white layer prevents the removal of carbon from the steel – a thin rim with a pearlite structure has formed at the border of the decarburized and white layers, Fig. 5, *e*. The decarburization zone is characterized by the development of recrystallization with the formation of columnar crystals. The microhardness of the white layer is 1.5 times higher than the microhardness of the main microstructure of the steel.

Electron probe microanalysis (Camebax Micro) revealed elements of copper and gold near the boundary with the cavity in the structures of cast iron and steel subjected to the action of plasma jets. These elements were not included in the initial composition of iron and steel. It is obvious that they were components of plasma jets.

Next mass spectroscopic analysis of the cast iron plug and steel target was carried out four years later. The appearance of a high concentration of the ^{55}Mn isotope was unexpected, since it was not detected during the first analysis either in the original metals or after the shock wave action. At the same time, the ^{55}Fe and ^{64}Cu isotopes were detected only in the first analysis near the boundary with the cavity formed by the action of the plasma jet.

Using the idea of our colleagues A. I. Lyuty & L. N. Glushko, let us explore one of the possible scenarios for the formation of multiply charged ions and estimate the change in the ionic composition of the substance as the converging shock wave moves depending on the charge number of atoms of the anode material. The formation of dissociated atoms is characterized by high mobility, which largely ensures high rates of physicochemical transformations and phase transitions [56].

For a fixed moment of time, the volumetric energy density in the front of a converging spherical shock wave $w(r)$ will be equal to

$$w(r) = w_0(r_0/r)^2, \quad (1)$$

where r_0 is the radius of a spherical target that takes on the impact of a powerful pulse of an electron beam accelerated in an electric field with an electric potential difference of several tens of kilovolts. The volumetric energy density at the moment of wave initiation in the metal $w(r_0)$ can be determined from the expression

$$w(r_0) = \rho_0 c^2 / 2 = E/2, \quad (2)$$

where ρ_0 is anode material density; $c = [E/\rho_0]^{1/2}$ is speed of sound in metal; E is Young's modulus.

The energy I_i required for i -fold ionization of an atom with charge number Z , as well as the average radii of the corresponding ions in the ground electronic state, are calculated using approximate methods of quantum mechanics [57]. For a one-electron ion, the exact values of the ionization potential can be obtained using the Bohr theory for the isoelectronic series of hydrogen

$$I_i = z = I_H Z^2, \quad (3)$$

where $I_H = 13.54$ eV is ionization potential of the hydrogen atom. In this case, the average distance of a single electron from the nucleus for an $i = (Z - 1)$ -fold ion is equal to

$$\langle r_{Z-1} \rangle = a_0/Z, \quad (4)$$

where a_0 is Bohr radius, $a_0 = 5.29 \cdot 10^{-11}$ m.

It should be noted that the one-electron ion of an atom is of particular interest, since the separation of the last electron from the nucleus transforms the “nucleus-electron” system into the state of nuclear plasma, whose particle radii are 4–5 orders of magnitude smaller than the dimensions of the initial neutral atom. The number of one-electron ions per unit volume of a substance can be estimated from the ratio

$$n_{Z-1} = \left[\frac{4\pi}{3} (\langle r_{Z-1} \rangle)^3 \right]^{-1} = \left[\frac{4\pi}{3} \frac{a_0^3}{Z^3} \right]^{-1}. \quad (5)$$

The volumetric energy density at a distance r from the centre of convergence of the shock wave, which is included in (1), will be equal to

$$w(r) = n_{Z-1} \sum_{i=1}^{Z-1} I_i. \quad (6)$$

Here $\sum_{i=1}^{Z-1} I_i$ is the sum of electron detachment energies from a neutral atom and a sequence of ions up to the multiplicity $i = Z - 1$.

When calculating $\sum_{i=1}^{Z-1} I_i$ for the first twenty chemical elements of the periodic system from hydrogen to calcium, the values of the ionization potentials of atoms and ions were used [58]. For more estimates than the specified amount within the periodic system, we can recommend the function

$$\sum_{i=1}^{Z-1} I_i = 3.715 \cdot Z^{2.72}, \quad (7)$$

obtained from the slope of the line and the length of the segment cut off by it on the y-axis.

Given calculations make it possible to estimate the distance r from the “focus” of the converging front of a spherical shock wave to the place where a single electron remains in the electron shell of the original atom. After the detachment of this electron, the system begins to shrink to the density of nuclear matter. From relations (1–7) one can obtain

$$r = 4.088 \cdot 10^{-16} \frac{c r_0 \rho_0^{1/2}}{Z^{2.86}}. \quad (8)$$

Figs. 6 and 7 show the plots of the dependence of the volume energy density w_0 , $\lg w$ on the neutral atom. The values of the sum of electron detachment energies $\lg \sum_{i=1}^{Z-1} I_i$ from the

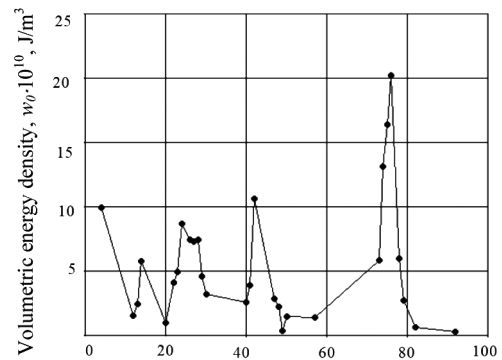


Fig. 6. Dependence of the volumetric energy density w_0 on the charge number of the atom

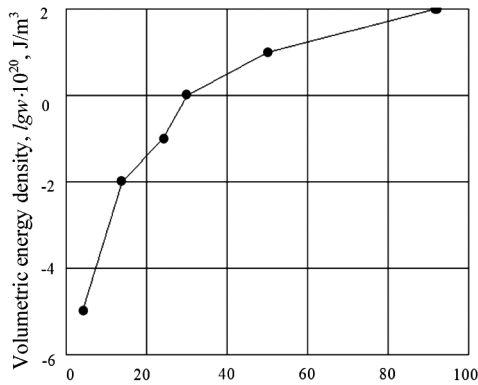


Fig. 7. Dependence of the volumetric energy density $\lg w$ on the charge of a neutral atom

charge number Z are shown in Fig. 8, where the indicated dependence is presented for chemical elements with the number $Z = 1 - 20$ and does not noticeably deviate from the linear character.

Fig. 9 for a number of metals shows the dependence of the distance r on Z calculated using expression (8). The calculation was carried out without taking into account the instability of the converging shock wave front, which arises when the wave front approaches the centre, which was observed in [59].

The nuclear radii r_n were calculated using the well-known formula

$$r_n = 1.3 \cdot 10^{-15} \cdot A^{1/3}, \quad (9)$$

where A is a mass number of the nucleus (sum of protons and neutrons). The calculation was made for $r_0 = 10^{-8}$ m [60].

Comparison of the values of r and r_n calculated from (8) and (9) shows that for heavy nuclei these values become close.

The volumetric energy density required to form a one-electron ion, increases monotonically as the charge number

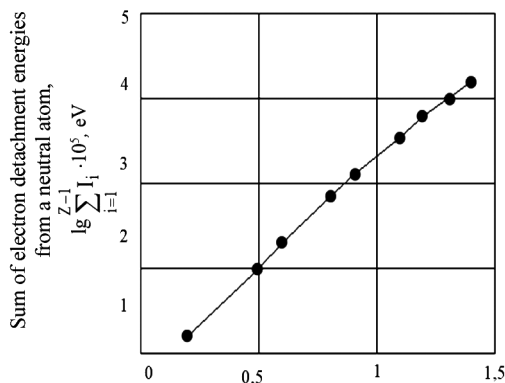


Fig. 8. Dependence of the sum of electron detachment energies from a neutral atom on the charge number

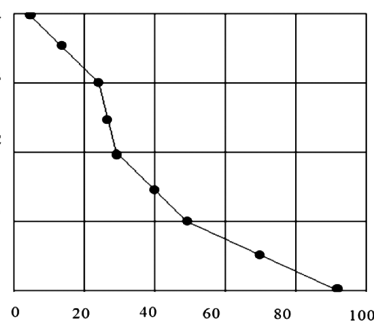


Fig. 9. The distance of an atom to the focus of a converging shock front as a function of the atomic charge

increases. Consequently, the smaller the charge number of a metal atom is, the sooner the “stripping” of electrons and the transformation of the plasma of a solid body into nuclear matter is completed. The last one is a mixture of positively charged metal nuclei and free electrons formed during the ionization of atoms or singly charged ions, initially located at the nodes of the crystal lattice.

The initial element of the plasma structure is a massive positive ion. Since it is surrounded by a dense cloud of free electrons, the high charge number of the nucleus is not an obstacle to the approach of the nuclei to a distance sufficient to enable nuclear forces. Here, both the decay reactions of heavy nuclei and the synthesis of superheavy components in the resulting plasma become possible.

Comparative analysis of calculating temperatures in [4, 14], the value of the temperature in this work and in a number of other similar experiments [13, 26, 31, 45] in order of magnitude ($1 \cdot 10^6 - 3 \cdot 10^6$ K) do not fundamentally differ. Studying the shock-wave parameters of substance in conical targets, the authors of [4, 14, 15, 45] note that, at close shock-wave parameters, but different geometries of conical targets and chemical composition of the substance, in particular, upon initiation of the D–D reaction, the generation of the neutron yield reaches 106 and even 1011 pulse⁻¹. In explosive plasma generators with a conical target, compression and heating of the substance in the target are carried out using a charge of a chemical explosive, while each of the values of the number of generated neutrons corresponds to a quite specific temperature range [4, 45]. In our experiments, neutron generation was not studied.

The temperature and density of the gaseous medium reach the highest values around the top of the cone during the collision of plasma flows behind the primary and secondary shock fronts of the Mach wave at the ultimate compression of substance under these conditions. The temperature of the plasma jet is $\sim 2.8 \cdot 10^6$ K, the calculated pressure upon impact of the jet on a metal sample reached 1120 GPa.

The spectra of ⁵⁵Fe, ⁵⁵Mn, ⁶⁴Cu isotopes were recorded in shock-compressed metals (cast iron, steel), Figs. 4 and 5. Pressing a metal plug into a conical cavity (according to [13, 14]) causes additional compression of the mixture of hydrogen isotopes and the yield of thermonuclear neutrons $\sim 10^4 - 10^{7.5}$ pulse⁻¹, which indicates a plasma temperature equal to $3 \cdot 10^6 - 10^7$ K. In this case, the features of the experimental scheme, hydrodynamic flows are the same as in [10, 15], i.e. using a metal striker sped up by the explosion products. In acute-angled geometry, (the angle at the top of the cone is 30–60°), the probability of occurrence of an irregular reflection of the shock wave in the air from the walls of the cone is insignificant. The angles of reflection of the shock wave front from the wall of the cone will be equal to 75–60°, while the irregular reflection of shock waves in air occurs at angles of 39–55° [42]. The reasons for the formation of experimentally detected isotopes can be as follows.

With a compressible spherical shock wave front in the material, the volumetric energy density increases rapidly [25]. This leads to the detachment of electrons from deeper atomic shells, which is accompanied by a sharp decrease in the volume of positive ions of increasing ionization multiplicity and a corresponding increase in temperature, pressure, and density of substance behind the shock wave.

With superstrong compression, an internal pressure about of several hundred megabars develops in the condensed substance, even in the absence of heating – only due to external influence and mutual repulsion of atomic nuclei. The existence of this pressure of non-thermal origin, which is completely uncharacteristic of gases, determines the main features of solids and liquid substances when they are compressed by shock waves [14].

As the shock compression pressure increases, the atomic repulsion energy increases and can reach the value of the dis-

sociation energy. From a physical point of view, this means that there is no minimum of the chemical bond energy on the potential curve [28]. Especially obvious is the dissociation of molecules with an increase in temperature due to distance increasing between atoms, but the opposite picture occurs during compression – the atoms approach each other. This contradiction is imaginary and can be explained easily. When the nuclei of atoms approach each other, deformation of the electron shells occurs, as a result of which valence electrons are displaced from the interatomic region – there is a transition of electrons from bound orbitals to loosening orbitals. Pashkov P.O. & Polyakova I.I. (1971) from the Volgograd Polytechnic Institute revealed that loosening orbits correspond to conduction bands in crystals. This state can correspond on the graphs to the point of intersection of the potential curve $E = f(R)$ with the axis R and which means the transition of a solid dielectric to a metallic state, in which there are no localized chemical bonds (Batsanov S.S., 1974) [56]. In this case, the atoms are dissociated formations immersed in an electron gas.

Descriptions of physical effects [19], which manifest themselves in a nanosecond pulsed discharge, have arguments to confirm both the first and second versions. The first of them is evidenced by the full spectrum of the elements of the periodic system, which arises when an anode of the selected metal is bombarded with high-energy electrons. The second version is confirmed by the nuclei of transuranium elements registered in the experiment. According to [11, 12, 19, 60], particles with mass numbers reaching $A \sim 4000$ were observed. The authors of these papers suggest that nuclei with mass numbers up to 10,000 were also produced. Theorists [61] also predicted the possibility of the existence of superdense nuclei. The synthesis of nuclei of transuranium elements correlates with an anomalously high concentration of protons, which, after relaxation of the nuclear plasma, become nuclei of the hydrogen atom. Neutrons predominate in the composition of the atomic nucleus in heavy elements. In the synthesis reaction of nuclei with a number of neutrons equal to the sum of these particles in the nuclei of positive ions that arise during the ionization of the initial atoms, a known excess of positive charges is obtained, which was observed in the form of the proton component of the resulting plasma.

In experiments [5, 11, 12, 20], the absence of radioactivity in the resulting material was noted after the collapse of the compression shock wave in the centre or near the axis [62], indicating that the described effect on matter brings it to the equilibrium state. We use the above assumptions about the causes and mechanisms of the formation of isotopes and chemical elements under the condition of a converging spherical or cylindrical front of a strong shock wave. One of the known methods for producing the iron-55 isotope is to irradiate the ^{56}Fe and ^{54}Fe isotopes with neutrons (Dwight D.J., Lorch E.A., Lovelock J.E. (1976). The ^{55}Fe isotope has a half-life of 2.737 years. The decay of this isotope occurs by capturing one orbital electron by a proton nucleus (one of the types of β -decay of atomic nuclei [17, 63]) and transformation into a stable isotope ^{55}Mn . As a result of e -capture, a pair of proton + electron turns into a neutron, emitting an electron neutrino, while the protons of the nuclei of multielectron elements can capture two orbital electrons.

Copper that arose on the surface of a conical depression corresponds to natural copper, consisting of two stable isotopes copper-63 and copper-65 [64]. It is interesting to consider the copper-64 isotope in an amount of about 1.5 %, found in the narrow zone of the cast iron microstructure adjacent to the surface of the crater formed by the impact of the plasma jet. Using the experience of mass spectroscopic studies on the radon content in iron target samples after explosive alloying [5], the studies on iron and copper isotopes were carried out 6 hours after explosive treatment. The chemical composition of the original cast iron does not contain copper. Possible sources of the copper-64 isotope could be a plasma jet con-

taining natural copper isotopes, a nickel-64 isotope, or both sources simultaneously. According to estimates, the mass of nickel, which can be involved in a plasma jet of significant penetration into cast iron, is about 0.0015 g, the mass of copper in the process of jet formation is 0.0011 g, i.e. similar values. The highest probability of the formation of the copper-64 isotope could occur at the moment of collision of dense plasma flows in the so-called plasma focus, in which there is an abrupt increase in temperature, concentration of ions and neutrons (D.P. Petrov, N.V. Filippov, T.I. Filippova, V.A. Khrabrov, 1958).

Conclusion. For the first time, the formation of oppositely directed symmetrical plasma jets during gas compression in conical targets has been experimentally observed. It is the first time that metal-physical studies of the microstructure of cast iron and steel have been carried out after the action of high-energy jets of dense high-temperature plasma $T = (2.5-2.8) \times 10^6$ K, and the pressure $P = 1.12 \cdot 10^{12}$ Pa arising from the collision of the jet with a barrier.

Iron-55 and copper-64 isotopes were found in the cast iron microstructure near the surface formed by the action of the plasma jet. The main components of the plasma jet were gaseous oxygen, nitrogen, argon, atomic iron, copper and gold. The fact of the formation of isotopes is the result of nuclear reactions. One of the main conditions for the implementation of such reactions is a dense high-temperature plasma. It is assumed that under the action of a strong shock wave in a conical target, in addition to the synthesis reaction, other nuclear reactions with heavy elements can be realized.

The physical concepts of the expected state of matter in a compression shock wave are presented, taking into account the change in the volumetric energy density at the moment of transformation of a solid body plasma into nuclear matter.

Acknowledgments. We cannot overemphasize the help in organizing and conducting experiments, in discussing the results obtained by Doctors of Physical and Mathematical Sciences A. Ye. Voytenko and E. G. Popov, Academician of the National Academy of Sciences of Ukraine Yu. N. Taran, Doctors of Technical Sciences Yu. I. Merezhko, S. I. Gubenko, S. M. Usherenko, Polish colleagues Karol Yach and Jan Ovsik, General Director of the Pavlohrad Chemical Plant, Doctor of Technical Sciences L. N. Shiman, Director of the Institute of High-Energy Materials, Doctor of Technical Sciences E. B. Ustimenko, employees of the Department of Physics of Dnipro University of Technology, Candidates of Physical and Mathematical Sciences A. I. Lyuty, L. N. Glushko and many others of our colleagues who sincerely shared their ideas, knowledge and rich experience in research, organizational and production activities.

References.

1. Inozemtseva, O. A., Voronin, D. V., Petrov, A. V., Petrov, V. V., Lapin, A. S., Kozlova, A. A., ..., & Gorin, D. A. (2019). Destruction of the shells of polymer and composite microcapsules under the action of high-intensity focused ultrasound. *Kolloidnyy zhurnal*, 81(1), 49-60. <https://doi.org/10.1134/S0023291219010075>.
2. Volkov, N. B., Mayyer, A. Ye., Talala, K. A., & Yalovets, A. P. (2006). On the mechanism of formation of microcraters on the surface of a target irradiated by a powerful electron beam. *Pis'ma v zhurnal tekhnicheskoy fiziki*, 32(10), 20-28.
3. Artemenko, I. I., Golovanov, A. A., Kostyukov, I. Yu., Kukushkina, T. M., Lebedev, V. S., Nerush, Ye. N., Samsonov, A. S., & Serebryakov, D. A. (2016). Plasma formation and dynamics in superstrong laser fields with allowance for radiation and quantum electrodynamic effects. *Pis'ma v Zhurnal eksperimental'noy i teoreticheskoy fiziki*, 104(12), 892-902. <https://doi.org/10.7868/S0370274X16240139>.
4. Sokolov, I. V. (1990). Hydrodynamic cumulative processes in plasma physics. *Uspekhi fizicheskikh nauk*, 160(11), 143-166.
5. Sobolev, V. V., & Usherenko, S. M. (2006) Shock-wave initiation of nuclear transmutation of chemical elements. *Journal De Physique*, IV: JP 134, August 2006, 977-982. <https://doi.org/10.1051/jp4:2006134149>.
6. Sobolev, V., Cabana, E. C., Howaniec, N., & Dychkovskiy, R. (2020). Estimation of Dense Plasma Temperature Formed under

- Shock Wave Cumulation. *Materials*, 13(21), 4923, 1-9. <https://doi.org/10.3390/ma13214923>.
7. Sobolev, V. V., Baskevich, A. S., Shiman, L. N., & Usherenko, S. M. (2016). Mechanism of thick metal walls penetration by high-speed microparticles. *Naukovyi Visnyk Natsionalnoho Hirnychoho Universytetu*, (6), 75-83.
 8. Usherenko, S. M. (1998). *Superdeep penetration of particles into barriers and creation of composite materials*. Minsk: NII IP s OP.
 9. Usherenko, S. M. (2001). Ideas about the effect of superdeep penetration. *Sbornik nauchnykh trudov Natsional'noy Gornoy Akademii Ukrainy*, 3(11), 13-23.
 10. Adamenko, S. V., Adamenko, A. S., & Vysotskii, V. I. (2004). Full-range nucleosynthesis in the laboratory Stable Superheavy Elements: Experimental Results and Theoretical Descriptions. *Infinite Energy*, 5(4), 1-8.
 11. Adamenko, A. S., Adamenko, S. V., & Bulyak, Ye. V. (2005). Experimental studies of a convergent density wave in a cylindrical anode of a high-current diode. *Pis'ma v zhurnal tekhnicheskoy fiziki*, 31(10), 24-29.
 12. Adamenko, S., Esaulov, A., Ulmen, B., Novikov, V., Ponomarev, S., Adamenko, A., ..., & Novikov, D. (2015). Exploring new frontiers in the pulsed power laboratory: Recent progress. *Results in Physics*, 3, 62-68. <https://doi.org/10.1016/j.rinp.2015.02.005>.
 13. Derentovich, G. (1989). Strong compression of matter by cumulating the energy of explosives. *Prikladnaya matematika i tekhnicheskaya fizika*, (4), 23-35.
 14. Anisimov, S. A., Bepalov, V. Ye., Vovchenko, V. I., Dromin, A. N., Dubovitskiy, F. I., Zharkov, A. P., ..., & Shur, L. N. (1980). Generation of neutrons upon explosive initiation of a D-D reaction in conical targets. *Pis'ma v zhurnal eksperimental'noy i teoreticheskoy fiziki*, 31(1), 67-70.
 15. Voytenko, A. Ye., & Sverdluchenko, B. V. (1989). Formation of a crater in a metal by an impact of a high-enthalpy plasma. *Prikladnaya mekhanika i tekhnicheskaya fizika*, (6), 19-22.
 16. Tsarov, V. A. (1990). Low-temperature nuclear synthesis. *Uspekhi fizicheskikh nauk*, 160(11), 1-53.
 17. Zel'dovich, Ya. B. (1985). *Selected works. Particles, nuclei, Universe*. Moscow: Nauka.
 18. Adamenko, S. V., Bereznyak, P. A., & Mikhaylovskiy, I. M. (2001). Initiation of an electric vacuum discharge by accelerated nanoparticles. *Pis'ma v zhurnal tekhnicheskoy fiziki*, 27(16), 15-20.
 19. Adamenko, S. V., Selleri, F., & Van der Merwe, A. (2007). *Controlled Nucleosynthesis. Breakthroughs in Experiment and Theory*. Series: Fundamental theories in Physics, 156(11). Springer.
 20. Ovchinnikov, V. I., Doroshkevich, Ye. A., Belous, A. I., Petlitskaya, T. V., Reut, O. P., & Usherenko, S. M. (2007). Effects of electromagnetic radiation observed under loading conditions with a high-energy flux of powder particles, (pp. 153-160). *Fizika i tekhnika vysokoenergeticheskoy obrabotki materialov*. Dnepropetrovsk: Art-Press.
 21. Marukovich, Ye. I., Usherenko, Yu. S., & Usherenko, S. M. (2021). *Dynamic modification of metals: monograph*. Minsk: Belaruskaya navuka.
 22. Adamenko, S. V., & Vysotskii, V. I. (2004). Evolution of Annular Self-controlled Electron-Nucleus Collapse in Condensed Targets. *Foundations of Physics*, 34, 1801-1831.
 23. Fleishmann, M., Pons, S., & Hawkins, M. (1989). Electrochemically induced nuclear fusion of deuterium. *Journal of Electroanalytical Chemistry*, 261, 301-308.
 24. Timashev, S. F. (2017). On the mechanisms of low-energy nuclear-chemical processes. *Radioelektronika, nanosistemy. Informatsionnyye tekhnologii (RENSIT)*, 9(1), 37-51. <https://doi.org/10.17725/rensit.2017.09.037>.
 25. Savvatimova, I. (2011). Transmutation of elements in low-energy glow discharge and the associated processes. *Condensed Matter Nuclear Science*, (8), 1-19.
 26. Voytenko, A. Ye., & Sobolev, V. V. (2012). On the estimation of the temperature of high-speed plasma jets formed in explosive generators. In *Shock waves in condensed media*, (pp. 238-246). Kyiv: Interpres LTD. Retrieved from http://ru.combex.org/conf_files/SWCM-2012.pdf.
 27. Sobolev, V. V., & Usherenko, S. M. (2008). Formation of chemical elements under superdeep penetration of lead microparticles in ferrous target. *Advanced Materials Research*, 47-50, part 1, 25-28. Hong Kong, P.R.; China. Retrieved from <https://www.scientific.net/AMR.47-50.25>.
 28. Sobolev, V. V., Bilan, N. V., Baskevich, A. S., & Stefanovich, L. I. (2018). Electrical charges as catalysts of chemical reactions on a solid surface. *Naukovyi Visnyk Natsionalnoho Hirnychoho Universytetu*, (4), 50-58. <https://doi.org/10.29202/nvngu/2018-4/7>.
 29. Timashev, S. F. (2015). Radioactive decay of nuclei as an initiated nuclear-chemical process: phenomenology. *Zhurnal fizicheskoy khimii*, 89(11), 1810-1822.
 30. Gubenko, S. I., Sobolev, V. V., & Slobodskoy, V. Ya. (1987). Structural changes in metal alloys treated with high-energy gas jets. In *Izmeneniye svoystv materialov pod deystviyem vysokikh davleniy*, (pp. 127-133). Kyiv: Institut problem materialovedeniya.
 31. Voytenko, A. Ye. (2001). On the question of the limiting temperature in explosive plasma generators. *Sbornik nauchnykh trudov Natsional'noy Gornoy Akademii Ukrainy*, 3(11), 5-9.
 32. Chernai, A. V., Sobolev, V. V., Chernaj, V. A., Ilyushin, M. A., & Dlugashek, A. (2003). Laser ignition of explosive compositions based on di-(3-hydrazino-4-amino-1,2,3-triazole)-copper(II) perchlorate. *Combustion, Explosion and Shock Waves*, 39(3), 335-339.
 33. Gerasimov, S. I., Ilyushin, M. A., Kuznetsov, P. G., Putis, S. M., Dushenok, S. A., & Rozhentsov, V. S. (2021). Initiation of Detonation by a Light Pulse in a Thin Charge of the VS-2 Pyrotechnic Composition. *Technical Physics Letters*, 47, 111-113. <https://doi.org/10.1134/S1063785021020048>.
 34. Sobolev, V. V., Taran, Y. N., & Gubenko, S. I. (1997). Shock wave use for diamond synthesis. *Journal De Physique*, 7(3), C3-73-C3-75. Retrieved from <https://hal.archives-ouvertes.fr/jpa-00255438>. Submitted on 1 Jan 1997.
 35. Chernaj, A. V., & Sobolev, V. V. (1995). Laser method of profiled detonation wave generation for explosion treatment of materials. *Fizika i Khimiya Obrabotki Materialov*, (5), 120-123.
 36. Sobolev, V. V., & Bilan, N. V. (2018). Physical conditions of the 'light' core formation and thermonuclear heat source deep inside the earth. *Naukovyi Visnyk Natsionalnoho Hirnychoho Universytetu*, (5), 13-23. <https://doi.org/10.29202/nvngu/2018-5/1>.
 37. Sobolev, V. V., Gubenko, S. I., Rudakov, D. V., Kyrychenko, O. L., & Balakin, O. O. (2020). Influence of mechanical and thermal treatments on microstructural transformations in cast irons and properties of synthesized diamond crystals. *Naukovyi Visnyk Natsionalnoho Hirnychoho Universytetu*, (4), 53-62. <https://doi.org/10.33271/nvngu/2020-4/053>.
 38. Al'tshuler, L. V., Trunin, R. F., Uurlin, V. D., & Fortov, V. Ye. (1999). Development in Russia of dynamic methods for studying high pressures. *Uspekhi fizicheskikh nauk*, 169(3), 323-344.
 39. Kanel', G. I., Fortov, V. Ye., & Razorenov, S. V. (2007). Shock waves in condensed matter physics. *Uspekhi fizicheskikh nauk*, 177(8), 809-830.
 40. Trunin, R. F. (Ed.) (1992). *Properties of condensed matter at high pressures and temperatures*. Arzamas: VNII eksperimental'noy fiziki.
 41. Kanel', G. I., Razorenov, S. V., Utkin, A. V., & Fortov, V. Ye. (1996). *Shock-wave phenomena in condensed media*. Moscow: Yanus-K.
 42. Orlenko, L. P. (Ed.) (2004). *Explosion physics (3rd ed.)* Moscow: Fizmatlit.
 43. Milyavskiy, V. V., Fortov, V. Ye., Frolova, A. A., Khishchenko, K. V., Charakhch'yan, A. A., & Shurshalov, L. V. (2010). On the mechanism of pressure increase with increasing porosity of media shock-compressible in conical and cylindrical targets. *Zhurnal vychislitel'noy matematiki i matematicheskoy fiziki*, 50(12), 2195-2207.
 44. Charakhch'yan, A. A., Khitsenko, K. V., Milyavskiy, V. V., Fortov, U. V., Frolova, A. A., Lomonosov, I. V., & Shurshalov, L. V. (2005). Numerical study of converging shock waves in porous media. *Zhurnal tekhnicheskoy fiziki*, 75(8), 15-25.
 45. Nemchinov, I. V., Trubetskaya, I. A., & Shuvalov, V. V. (1984). Explosion in a limited volume of gas under strong radiation. *Prikladnaya matematika i tekhnicheskaya fizika*, (6), 108-112.
 46. Nedostup, V. I., & Gal'kevich, Ye. P. (2000). Equations of state for helium, hydrogen, deuterium, nitrogen, oxygen, carbon monoxide, carbon dioxide, methane at high temperatures and pressures. *Teplotekhnika vysokikh temperatur*, 38(3), 397-401.
 47. Bogdanov, E. N., Zhernokletov, M. V., Kozlov, G. A., & Rodionov, A. V. (2020). Study of shock-compressed argon plasma using microwave diagnostics. *Combustion, Explosion, and Shock Waves*, 56(4), 479-485. <https://doi.org/10.1134/S0010508220040127>.
 48. Fortov, V. Ye. (1982). Dynamic methods in plasma physics. *Uspekhi fizicheskikh nauk*, 138(3), 361-412. Retrieved from <https://docplayer.com/78969182-Uspehi-fizicheskikh-dinamicheskie-metody-v-fizike-plazmy-v-e-fortov.html>.
 49. Kondrikov, B. N., & Sumin, A. I. (1987). The equation of state of gases at high pressure. *Fizika gorennya i vzryva*, (1), 114-122.
 50. Mader, S. L. (1998). *Numerical Modeling of Explosives and Propellants (2nd ed.)*. CRC Press.
 51. Zel'dovich, Ya. B., & Rayzer, Yu. P. (2008). *Physics of shock waves and high-temperature hydrodynamic phenomena*. Moscow: Fizmatlit.

52. Ogorodnikov, V. A., Mikhaylov, A. L., & Burtsev, V. V. (2009). Registration of particle ejection from the free surface of shock-loaded specimens. *Zhurnal eksperimental'noy i teoreticheskoy fiziki*, 136(9), 1-9.
53. Sobolev, V., & Hove, I. Hogset (1997). Phenomenon of spiral vortex formation over the shock wave front. *Journal De Physique*, IV, 7(3), 127-129. Retrieved from <https://hal.archives-ouvertes.fr/jpa-00255481>.
54. Romanov, G. S., & Urban, V. V. (1982). Numerical simulation of an explosive plasma generator taking into account radiation energy transfer and wall evaporation. *Inzhenerno-fizicheskiy zhurnal*, 43(6), 1012-1019. Retrieved from http://www.itmo.by/publications/jepeter/bibl/?ELEMENT_ID=11682.
55. Danilenko, V. V. (2010). *Explosion: physics, technique, technology*. Moscow: Energoatomizdat.
56. Butyagin, P. Yu. (1984). Structural softening and mechanochemical reactions in solids. *Uspekhi khimii*, 53(2), 1769-1789.
57. Landau, L. D., & Lifshits, Ye. M. (2012). *Quantum mechanics*. Moscow: Nauka.
58. Voronin, A. I., & Oshero, V. I. (1990). *Dynamics of molecular reactions*. Moscow: Nauka.
59. Zababakhin, Ye. I., & Zababakhin, I. Ye. (1988). *The phenomenon of unlimited cumulation*. Moscow: Nauka.
60. Antsyferov, P. S., & Dorokhin, L. A. (2017). Scaling of a fast spherical discharge. *Plasma Physics Reports*, 43(2), 164-169.
61. Sobolev, V. V., Skobenko, O. V., Usyk, I. I., Kulivar, V. V., & Kurliak, A. V. (2021). Formation of converging cylindrical detonation front. *Naukovyi Visnyk Natsionalnoho Hirnychoho Universytetu*, (6), 49-56. <https://doi.org/10.33271/nvngu/2021-6/049>.
62. Pujol, M., Marty, B., Burnard, P., & Philippot, P. (2009). Xenon in Archean barite: Weak decay of ^{130}Ba , mass-dependent isotopic fractionation and implication for barite formation. *Geochimica et Cosmochimica Acta*, 73, 6834-6846. <https://doi.org/10.1016/j.gca.2009.08.002>.
63. Aprile, E., Aalbers, J., & Agostini, F. (2019). Observation of two-neutrino double electron capture in ^{124}Xe with XENON1T. *Nature*, 568, 532-535. <https://doi.org/10.1038/s41586-019-1124-4>.
64. Tiba, A., Yegorov, A. Yu., Berdnikov, Ya. A., & Lomasov, V. N. (2021). Copper-64 isotope production through the cyclotron proton irradiation of the natural-nickel target. *Nauchno-tehnicheskkiye vedomosti SPbGPU. Fiziko-matematicheskkiye nauki*, 14(1), 138-146. <https://doi.org/10.18721/JPM.14110>.

Про механізм іонізації атомів при стискуванні речовини фронтом збіжної ударної хвилі

*В. В. Соколев¹, С. М. Ганєєв¹, О. В. Скобенко¹,
В. В. Кулівар¹, А. В. Курляк²*

1 – Національний технічний університет «Дніпровська політехніка», м. Дніпро, Україна, e-mail: velo1947@ukr.net
2 – Державне підприємство «Науково-виробниче об'єднання «Павлоградський хімічний завод», м. Павлоград, Дніпропетровська обл., Україна

Мета. Встановити зміни в мікроструктурі металів після впливу високоенергетичних струменів плазми, сформованих кумуляцією газодинамічних течій у конічній мішені. Провести оцінку передбачуваного стану речовини в сильній ударній хвилі стиснення з урахуванням зміни об'ємної щільності енергії в момент перетворення плазми твердого тіла в ядерну матерію.

Методика. Використані методика лазерного ініціювання профільованого фронту детонаційних хвиль у зарядах вибухових речовин і відповідного профілю ударних хвиль у матеріалах, методи й техніка вимірювання динамічних параметрів ударно-стислих речовин.

Результати. Проведене експериментальне дослідження фізико-хімічного стану речовини, обробленої екстремально високими тисками й температурами при стисканні ударними хвилями, що сходяться в конічних мішенях. Проаналізовані наукові результати фізико-математичного моделювання ударних хвиль, що сходяться.

Наукова новизна. Уперше експериментально виявлено утворення симетричних плазмових струменів при стисканні газу в конічних мішенях. Уперше проведені металофізичні дослідження мікроструктури чавуну та сталі після дії високоенергетичних струменів щільної плазми, що має температуру $(2,5-2,8) \cdot 10^6$ К, та тиску, який виникає під час зіткнення струменя з перешкодою $1,12 \cdot 10^{12}$ Па. У мікроструктурі чавуну поблизу поверхні, утвореної дією струменя плазми, виявлені ізотопи заліза-55 і міді-64. Основними компонентами плазмового струменя були газоподібний кисень, азот, аргон, в атомарному стані залізо, мідь і золото. Факт утворення ізотопів – результат ядерних реакцій. Однією з головних умов реалізації таких реакцій є щільна високотемпературна плазма. Передбачається, що під час дії сильної ударної хвилі в конічній мішені можуть бути реалізовані крім реакції синтезу ще й інші ядерні реакції з важкими елементами. Викладено уявлення про передбачуваний стан речовини в ударній хвилі стиснення з урахуванням зміни об'ємної щільності енергії в момент перетворення плазми твердого тіла в ядерну матерію.

Практична значимість. Практичне значення має запропонована методика проведення експериментальних досліджень ударно-стисненої речовини під дією екстремальних значень температури й тиску в мішені конічної форми із застосуванням засобів лазерного ініціювання хімічних вибухових речовин. Також важливим є уявлення про передбачуваний стан речовини в ударній хвилі.

Ключові слова: вибух, ударна хвиля, конічна мішень, термоядерна температура, плазма, ізотопи, ядерні реакції

The manuscript was submitted 10.08.21.